

Theoretical Investigations into Self-Organized Ordered Metallic Semi-Clusters Arrays on Metallic Substrate

Xiao-Chun Wang · Han-Yue Zhao ·

Nan-Xian Chen · Yong Zhang

Received: 24 January 2010 / Accepted: 29 March 2010 / Published online: 13 April 2010
© The Author(s) 2010. This article is published with open access at Springerlink.com

Abstract Using the energy minimization calculations based on an interfacial potential and a first-principles total energy method, respectively, we show that $(2 \times 2)/(3 \times 3)$ Pb/Cu(111) system is a stable structure among all the $[(n - 1) \times (n - 1)]/(n \times n)$ Pb/Cu(111) ($n = 2, 3, \dots, 12$) structures. The electronic structure calculations indicate that self-organized ordered Pb semi-clusters arrays are formed on the first Pb monolayer of $(2 \times 2)/(3 \times 3)$ Pb/Cu(111), which is due to a strain-release effect induced by the inherent misfits. The Pb semi-clusters structure can generate selective adsorption of atoms of semiconductor materials (e.g., Ge) around the semi-clusters, therefore, can be used as a template for the growth of nanoscale structures with a very short periodic length (7.67 Å).

Keywords Self-organized · Template · Interface potential · Molecular dynamics · First-principles calculation

Introduction

The microelectronics industries have refined the fabrication methods to make ever smaller devices, but these methods will soon reach their fundamental limits. A promising alternative way for the fabrication of nanometer functional

systems is to grow self-organized atoms and molecules on well-defined surface templates with periodic structures. This idea is of great interest not only for its promising applications in technology but also for a fundamental study [1–7]. When the mechanisms controlling the self-organized phenomena are fully disclosed, the self-organized growth processes can be steered to create a wide range of surface nanostructures from metallic, semiconducting and molecular materials. Theoretically, the energetic driving forces for self-organization have been explained by various mechanisms, such as overlapping electric [8], magnetic [9], and bulk elastic strain fields [10, 11]. However, many of these systems are too complex to predict a new self-organized structure with sufficient accuracy. Besides, as far as we know, there are only a few first-principles studies on the self-organization template because the experimentally observed super cells are too large to perform such a time-consuming calculation, such as Cu bilayer on Pt(111) and Ag bilayer on Pt(111) with (25×25) super cells [2]. Recently, the ordered arrays of clusters on metallic substrate are reported experimentally [12, 13]. As the substrate of the ordered clusters, the self-organized template plays a vital role in the growth process of the ordered clusters arrays. Indeed, the detail properties of these self-organization phenomena need thoroughly theoretical research, such as the structure property of the first adsorbing layer under the second layer in metal-bilayer/metal(111) system, because they cannot be observed directly in experiment. Our previous works focused on the behavior of identical metallic clusters arrays on the clean metallic or clean semiconductor substrate [3, 4]. Now, we turn to the self-organized metallic substrate with metal-bilayer/metal(111) structure, which can be used as a template.

In this paper, we apply two methods to perform energy minimization respectively on a series of complex

X.-C. Wang (✉) · H.-Y. Zhao · N.-X. Chen
Department of Physics, Tsinghua University,
100084 Beijing, People's Republic of China
e-mail: wangxiaochun@tsinghua.org.cn

Y. Zhang
Department of Electrical and Computer Engineering and Center
for Optoelectronics, The University of North Carolina
at Charlotte, Charlotte, NC 28223-0001, USA

Pb/Cu(111) interfaces with $[(n - 1) \times (n - 1)]/(n \times n)$ ($n = 2, 3, \dots, 12$) super cells to search a stable template and study its atomic and electronic structures. The two methods are molecular dynamics (MD) method based on Chen–Möbius inversion interfacial potential [14–18] and self-consistent first-principles method. Some experiments described a method to create almost monodisperse, equally spaced nanostructures through the self-organization of a fcc metal film on fcc metal (111) substrates with a periodic strain-relief template [2]. The nanostructures are stable, which are partly due to that the fcc metal (111) surface is a very stable surface with a very low surface energy [19]. Recently, there are increasing experiments studying the system of Pb atoms deposited on Cu(111) surface using the low-energy electron microscope (LEEM) and the scanning tunneling microscopy (STM) [20]. But as far as we know, very little theoretical study has been performed on the structure of Pb bilayer on Cu(111) surface. The lattice constant misfit ratio (37.1%) between Pb and Cu is very large, so the achievable periodicity of the Pb/Cu(111) template can be very short, if the system is stable. Thus, it will be easy to perform further theoretical study on the stable template with a very high density periodic structure, which may reveal important information for potential applications, e.g. in the high-density memory, catalysis or developing nanostructured device technology. In this paper, we identify a stable template of Pb bilayer on Cu(111) surface with a periodic nanometer structure and reveal the atomic and electronic structure properties of the template.

Calculation Method

In order to study the stability of the Pb/Cu(111) interface structures with misfit, the proper interfacial potentials are developed with Chen–Möbius lattice inversion method [14–18], and then the potentials are applied to relax the interface structures with energy minimization method in Cerius2 software package. The interface structures are modeled in super cells of $[(n - 1) \times (n - 1)]/(n \times n)$ Pb/Cu(111) ($n = 2, 3, \dots, 12$) to take the misfit into account. The $(n - 1) \times (n - 1)$ indicates the lateral super cell size of the Pb bilayer, and the $(n \times n)$ is for the super cell of Cu(111) substrate. The periodic length of the stable Pb/Cu(111) system is expected to be around the lease common multiple of the lattice constants of Pb and Cu. The $[(n - 1) \times (n - 1)]/(n \times n)$ super cells with the increasing value of n will be easy to meet the lease common multiple condition.

The Cu(111) surface is modeled by repeated slabs with five Cu layers separated by a vacuum region equivalent to twelve Cu layers. Each metal layer in the super cell

contains $n \times n$ Cu atoms that form a $(n \times n)$ surface cell. Two Pb bilayers are adsorbed symmetrically on both sides of the Cu slab. Such a super cell can well simulate the system of Pb bilayer on the Cu(111) surface, including a good description of the interaction between the two sides of the interface. All the Cu atoms are initially located at their bulk positions with the equilibrium lattice constant 3.61 Å. Upon Pb bilayer adsorptions, all the atoms in the unit cell except for the central Cu layer are fully relaxed. The Pb atoms in the Pb bilayer are also initially located at their bulk positions with the equilibrium lattice constant 4.95 Å. The same super cell models are used for the following first-principles calculations.

Then, for the stable structures that are found with energy minimization method based on the interfacial potentials, the first-principles calculations are carried out on these stable structures, which is based on a density functional theory implemented in a projector augmented wave (PAW) representation [21–23]. The exchange–correlation effect is treated with the generalized gradient approximation (GGA) [24, 25]. The plane wave kinetic energy cutoff employed is 25.73 Ry, and the Monkhorst–Park k -point mesh is $2 \times 2 \times 1$ [26]. The total energy convergences with respect to the energy cutoff and the number of k points have been tested. Optimizations of the atomic structures are done by the conjugate-gradient technique, using the calculated Hellmann–Feynman forces as guidance [27]. All the atomic geometries are fully relaxed, except the fixed center Cu layer, till the forces on all relaxed atoms are less than 0.01 eV/Å.

Results and Discussions

The interface system is totally different from bulk system, and then the potentials for bulk system are not applicable for the interfacial system. It is necessary to develop proper potentials for the interfacial system. The interaction potential $\Phi_{\text{Cu–Pb}}$ is extracted from first-principles cohesive energies, using the Chen–Möbius inversion method [14, 15]. The potentials $\Phi_{\text{Cu–Cu}}$ and $\Phi_{\text{Pb–Pb}}$ are extracted using the method in [18]. All the three potentials are expressed in the form of Rahman–Stillinger–Lemberg function:

$$\Phi = D_0 e^{y \left(1 - \frac{r}{R_0} \right)} + \frac{a_1}{1 + e^{b_1(r - c_1)}} + \frac{a_2}{1 + e^{b_2(r - c_2)}} + \frac{a_3}{1 + e^{b_3(r - c_3)}}. \quad (1)$$

The values of the parameters for the interaction potentials $\Phi_{\text{Cu–Pb}}$, $\Phi_{\text{Cu–Cu}}$ and $\Phi_{\text{Pb–Pb}}$ are shown in Table 1. Using these potentials, the lattice constants of bulk Cu and Pb are calculated, respectively, to be 3.61 and 4.95 Å, which consist well with the values of 3.61 Å in

Table 1 The parameters of $\Phi_{\text{Cu-Pb}}$, $\Phi_{\text{Cu-Cu}}$ and $\Phi_{\text{Pb-Pb}}$ for the Pb bilayer/Cu(111) structure

Pb/Cu(111)	D_0 (eV)	R_0 (\AA)	y	a_1 (eV)	b_1 (\AA^{-1})	c_1 (\AA)	a_2 (eV)	b_2 (\AA^{-1})	c_2 (\AA)	a_3 (eV)	b_3 (\AA^{-1})	c_3 (\AA)
$\Phi_{\text{Cu-Pb}}$	53.04	1.00	1.74	45.42	8.56	0.01	-4.95	1.56	2.21	-2.62	2.88	2.34
$\Phi_{\text{Cu-Cu}}$	626.96	1.00	0.50	4082.02	3.42	0.73	-476.68	0.50	1.62	-669.59	1.00	1.04
$\Phi_{\text{Pb-Pb}}$	370.36	1.00	1.02	4082.02	2.64	1.09	-476.68	1.05	1.02	-669.59	1.33	0.17

Ref. [28] and 4.949 \AA in Ref. [29]. These results indicate that the interaction potentials $\Phi_{\text{Cu-Cu}}$ and $\Phi_{\text{Pb-Pb}}$ are accurate to describe the interatomic interactions of Cu and Pb, respectively. Figure 1 shows the average energies per atom for the $[(n - 1) \times (n - 1)]/(n \times n)$ Pb/Cu(111) ($n = 2, 3, \dots, 12$) structures, which are calculated using the energy minimization calculation based on the interfacial potential. The average energy means that the total energy of each relaxed structure is divided by the total number of atoms in the same structure. When n varies from 5 to 12, the Pb bilayer does not remain in the bilayer structure but reorganize into three or even more layers and become disordered due to the increasing misfit strain. Therefore, these $n \geq 5$ structures cannot be used as stable templates to support ordered arrays of atoms or clusters. However, when $n < 5$, the relaxed structures retain the well-ordered two Pb layers on the Cu(111) substrate. These facts mean that $n = 5$ (i.e. $4 \times 4/5 \times 5$) is a critical case. When $n = 4$ (i.e. $3 \times 3/4 \times 4$), each layer of the Pb bilayer completely covers the Cu surface at 0.56 ML (here, 1 ML is defined as one Pb atom per surface Cu atom) with the lattice constant close to $4/3$ that of the Cu. This result is consistent well with the experimental data [20]. The average energy of the $n = 3$ is slightly lower than that of $n = 4$, so the $(2 \times 2)/(3 \times 3)$ Pb bilayer/Cu(111) is more stable than the structure of $n = 4$, while both structures of $n = 4$ and $n = 3$ are stable. When $n = 2$, the Pb surface cell will be 1×1 , it is not suitable to be used as a template for selective adsorptions of atoms or clusters.

Now, we carry out a comprehensive study on the atomic and electronic properties of the stable $(2 \times 2)/(3 \times 3)$ and $(3 \times 3)/(4 \times 4)$ Pb/Cu(111) structures with first-principles calculations. For the $(2 \times 2)/(3 \times 3)$ structure, Fig. 2a shows the top view of the fully relaxed structure. In each super cell (marked with the green bigger parallelogram), the four Pb atoms of the second Pb layer form a relatively close packed semi-cluster structure. Here, we define the semi-cluster as a kind of structure exhibiting the cluster character only in 2-D plane (in the (111) surface plane for this paper). The ordered semi-clusters divide the surface into two kinds of areas. One is the area within semi-cluster; the other is the area between neighboring semi-clusters. The two areas have different character, which will lead to selective adsorption for atoms or clusters. For the second Pb layer, the nearest distance of the Pb atoms is 3.60 \AA (but

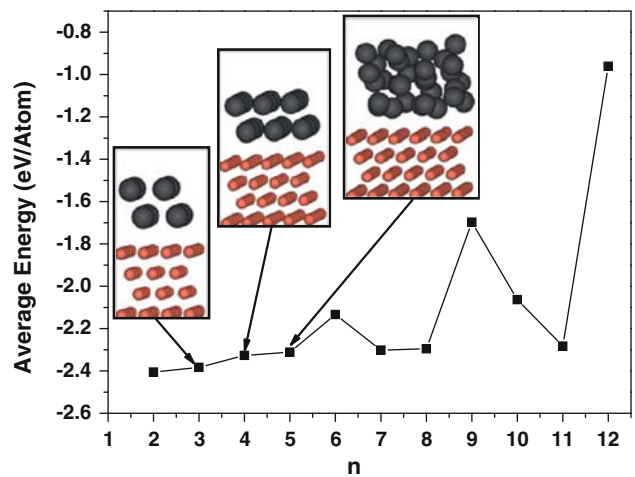


Fig. 1 The average energies for the $[(n - 1) \times (n - 1)]/(n \times n)$ Pb bilayer/Cu(111) ($n = 2, 3, \dots, 12$) structures. The dark (big) and red (small) balls are for Pb and Cu atoms, respectively

3.75 \AA for the first Pb layer) that is shorter than that of 4.06 \AA (3.90 \AA) between neighboring semi-clusters by 0.46 \AA (0.15 \AA). The semi-cluster is induced by misfit strains between the Pb and Cu atoms at the interface. This fact indicates that within the semi-cluster, the Pb atoms are closer and have stronger interaction than that between the neighboring semi-clusters. Figure 2b shows the relative sites of all Pb and Cu atoms. These atoms in $(2 \times 2)/(3 \times 3)$ Pb/Cu(111) structure are shifted into one Cu(111) (1×1) surface cell, but retain their relative positions. The “A”, “B” and “C” points denote the Cu atoms in the central, upper and top Cu layers of the slab respectively, which are the standard fcc sites. One of the blue triangles that correspond to the first Pb layer locates at the upper corner that is equivalent to “A” site that belongs to fcc site relative to the top Cu layer. The other one blue triangle is near the “C” site. Another two blue triangles are near the borderline to form the transition area that can release the misfit strains. These facts indicate: (1) there is a strong interaction between the first Pb layer and the Cu substrate, which shortens the distance between the neighboring Pb semi-clusters in the first Pb layer; (2) the interaction between the Cu substrate and the first Pb layer is different from the interaction between the first and second Pb layers. Finally, these different interactions arrange the atoms in first Pb layer in a balance state.

Fig. 2 **a** Top view of the relaxed $(2 \times 2)/(3 \times 3)$ Pb/Cu(111) structure, and the green bigger parallelogram indicates one super cell. **b** The relative positions of Pb and Cu atoms in Cu(111) 1×1 surface cell for the same structure as (a). The black dot, blue triangle and red square are for the atoms of Cu substrate, first Pb layer and second Pb layer, respectively. The distances (\AA) between some Pb atoms are also shown

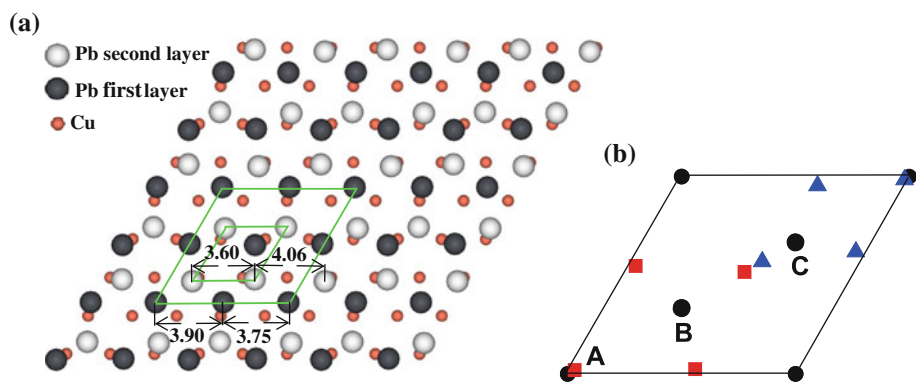
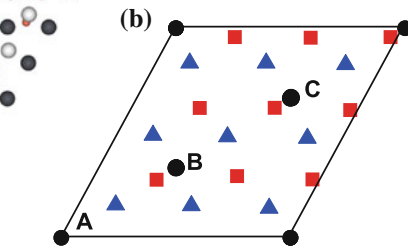


Fig. 3 **a** Top view of the relaxed $(3 \times 3)/(4 \times 4)$ Pb/Cu(111) structure, and the green parallelogram indicates one super cell. **b** The relative positions of Pb and Cu atoms in Cu(111) 1×1 surface cell for the same structure as (a). The black dot, blue triangle and red square are for the atoms of Cu substrate, first Pb layer and second Pb layer, respectively. The distances (\AA) between some Pb atoms are also shown

Figure 3a shows the top view of the fully relaxed structure of the $(3 \times 3)/(4 \times 4)$ Pb/Cu(111) structure. Contrast to the $(2 \times 2)/(3 \times 3)$ Pb/Cu(111) structure, the fcc area and hcp area for the first Pb layer in $(3 \times 3)/(4 \times 4)$ structure can be clearly seen in Fig. 3a. In this case, the fcc and hcp sites mean that the Pb atom of the first layer locates near the hollow site of the regular and inverted triangles made by three Cu surface atoms, respectively. There is a very clear borderline (green dashed) between the fcc and hcp areas. The three Pb atoms on the straight borderline locate near the bridge sites of the Cu(111) surface, and these three Pb atoms form the transition area between the fcc and hcp areas to release the misfit strains at the interface. Compared with the $(2 \times 2)/(3 \times 3)$ Pb/Cu(111) structures, the separation of the Pb atoms in the first layer are almost equal (around $3.41 \pm 0.04 \text{\AA}$) in the $(3 \times 3)/(4 \times 4)$ Pb/Cu(111) structure of Fig. 3a, which can be seen clearly in Fig. 3b. For the second Pb layer, the configuration of these Pb atoms is similar to those in the first Pb layer. Because the differences in the inter-atomic distances for the Pb atoms in second Pb layer are small (less than 0.1\AA), the surface of the Pb bilayer can be regarded as the clean Pb(111) surface in some degree for the adsorption atoms. This fact is due to



square are for the atoms of Cu substrate, first Pb layer and second Pb layer, respectively. The distances (\AA) between some Pb atoms are also shown

that the Pb atoms fully cover the Cu(111) surface and then they are closely packed. In other words, for the new adsorption atoms, Pb atoms in the second layer are almost identical. As a result, each hollow site in the Pb second layer will have equal chance to hold the deposited atoms, and the same thing would happen to each top and bridge site. Hence, the $(3 \times 3)/(4 \times 4)$ Pb/Cu(111) structure is not a suitable candidate to be used as a template.

Figure 4 shows the differences of electron charge densities for the $(2 \times 2)/(3 \times 3)$ Pb/Cu(111) structure, in order to see the nature of interaction between the Pb bilayer and the Cu(111) substrate, and the interaction between Pb atoms in Pb bilayer. The difference of electron charge density helps to visualize the characteristics of bonding and is defined as the differences between the Pb/Cu(111) structure and the superposition of atomic electron charge densities, i.e., $\Delta\rho_1(\vec{r}) = \rho(\text{Pb/Cu}(111)) - \sum_{\mu} \rho_{\text{atom}}(\vec{r} - \vec{R}_{\mu})$. In Fig. 4a, there are obvious covalent bondings between Pb atoms in first Pb layer and the Cu atoms at Cu(111) surface, which indicate the strong interactions between them. In the second Pb layer, there are alternatively high and zero electronic charge density areas between Pb atoms. Such a picture reveals that the direct interactions between these Pb atoms are alternatively strong and weak. Figure 4b shows a

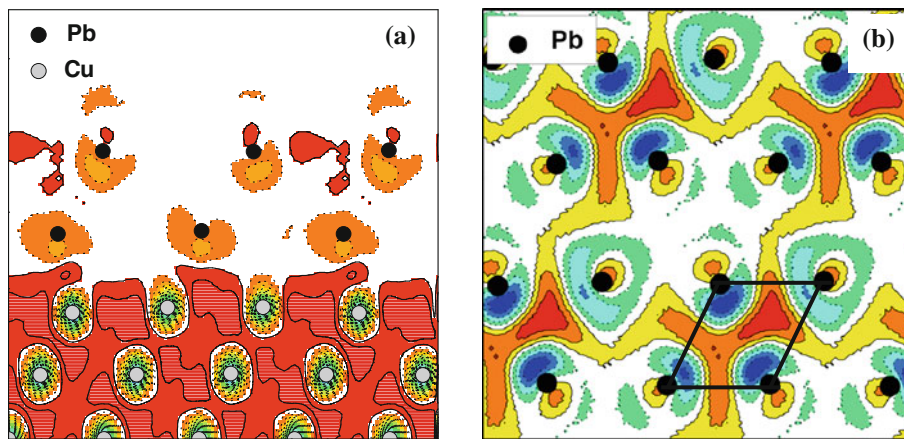


Fig. 4 **a** $\Delta\rho_1(\vec{r})$ for the $(2 \times 2)/(3 \times 3)$ Pb/Cu(111) structure, and the plotted plane is vertical to the Cu(111) surface and along the longer diagonal of the parallelogram pattern (in Fig. 2a); **b** the same as **a**, but the plotted plane is parallel to the Cu(111) surface and

very clear picture of the difference of the electron charge density in the second Pb layer. Each Pb semi-cluster (shown as a parallelogram in Fig. 4b) forms the area with a high charge density and is surrounded by the zero charge density area. The semi-clusters are separated by the dipole repulsion caused by elastic interactions due to the strain-relief of the lattice misfit in the interface. The atoms that will be deposited on the surface of $(2 \times 2)/(3 \times 3)$ Pb/Cu(111) structure will have different interactions with the two different areas. Such mechanisms will help to realize the selective adsorption of atoms on the surface of Pb bilayer/Cu(111). So the periodic $(2 \times 2)/(3 \times 3)$ Pb/Cu(111) structure will be a promising candidate for new self-organized template. Furthermore, the periodic length of this $(2 \times 2)/(3 \times 3)$ Pb bilayer/Cu(111) structure is 7.67 Å, which is very short for self-organized template. Therefore, this structure may be a unique template for growing ordered quantum dots with a very high density.

As for the $(3 \times 3)/(4 \times 4)$ Pb/Cu(111) structure, the differences of electron charge densities are shown in Fig. 5. The alternatively high and zero electronic charge density areas, which are found in $(2 \times 2)/(3 \times 3)$ Pb/Cu(111) structures, do not appear in $(3 \times 3)/(4 \times 4)$ structure. The electronic structures of Pb layers (shown in Fig. 5a, b) are hardly affected by the Cu substrate, and very similar to clean Pb (111) surface with (1×1) periodical cell. The electron charge density areas between neighboring Pb atoms along the Pb layer are almost same, because the Pb atoms are close packed along the (111) surface due to that the Pb over layer completely covers the Cu(111) surface in the $(3 \times 3)/(4 \times 4)$ structure. The $(3 \times 3)/(4 \times 4)$ Pb/Cu(111), which shows almost (1×1) surface electronic structure, is not suitable to be used as a template.

crossing the Pb atoms in the second layer. Solid lines (red area indicates highest value) and dashed lines (blue area indicates lowest value) correspond to $\Delta\rho > 0$ and $\Delta\rho < 0$, respectively. The white area corresponds to $\Delta\rho = 0$

As a test, we perform the first-principles calculations for the Ge atom adsorption on the $(2 \times 2)/(3 \times 3)$ Pb/Cu(111) template. The structures with Ge atoms adsorbing on the top and bridge sites of Pb bilayer are unstable. There are eight possible hollow sites for adsorption within one surface supercell of this stable template (Fig. 6a). The full relaxations are performed on these eight adsorption systems respectively. In Fig. 6b, the total energies of eight adsorption systems show that the sites S3 (representing the site 3 in Fig. 6a), S4 and S6 have lower total energy than the other sites. This fact implies that experimentally the Ge atoms will prefer to adsorb on the S3, S4 and S6 sites. Figure 6c shows that the binding energies of these three adsorption sites on $(2 \times 2)/(3 \times 3)$ Pb/Cu(111) are higher than the other sites. The lower total energies and higher binding energies of the S3, S4 and S6 adsorption sites will realize the selective adsorption of Ge atoms on $(2 \times 2)/(3 \times 3)$ Pb/Cu(111). It confirms that the $(2 \times 2)/(3 \times 3)$ Pb/Cu(111) is a promising candidate to be used as a periodic template to support ordered arrays of atoms. During an actual deposition process, if one Ge atom lands on the S1, S2, S5, S7 or S8, under a moderate temperature, the Ge atom could get enough energy to overcome a diffuse barrier and fall into the neighboring sites of lower total energy, for instance transferring from S5 to S4 or S6. Furthermore, it is necessary that the deposited Ge atoms should cover the surface of $(2 \times 2)/(3 \times 3)$ Pb/Cu(111) in a range from 0.11 to 0.33 ML. The right coverage of Ge atoms will contribute to the realization of an ordered arrangement of Ge atoms on the $(2 \times 2)/(3 \times 3)$ Pb/Cu(111) surface. Therefore, under an appropriate growth temperature and with careful control of the deposition rate, the adsorption of ordered Ge atoms on the surface of $(2 \times 2)/(3 \times 3)$ Pb/Cu(111) should be possible.

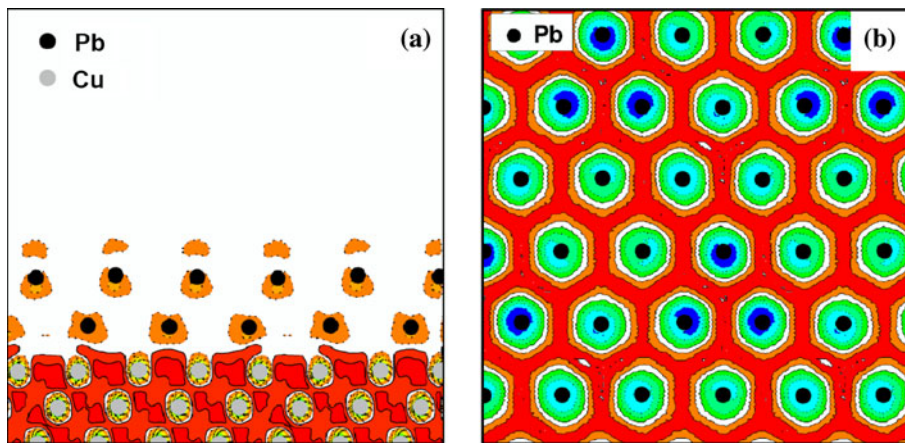
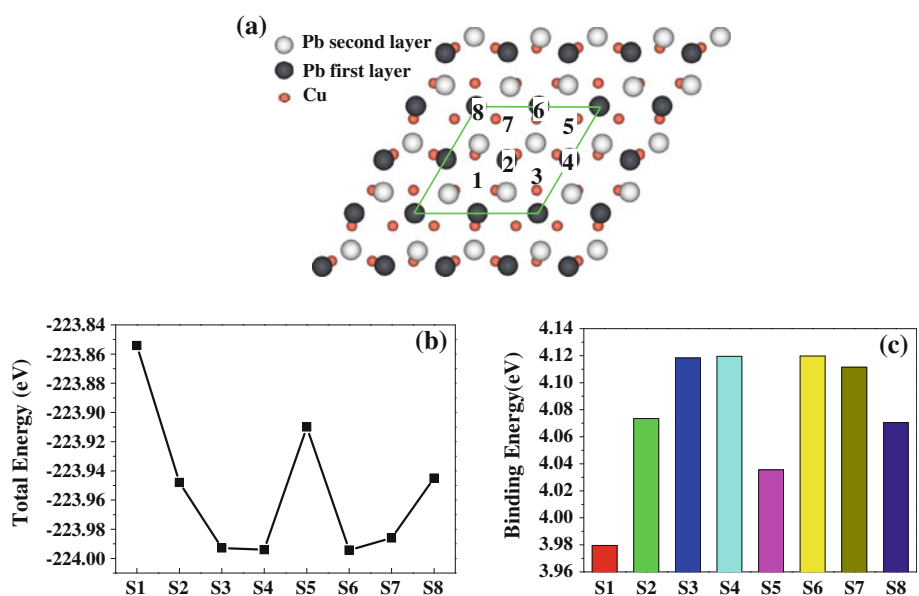


Fig. 5 **a** $\Delta\rho_1(\vec{r})$ for the $(3 \times 3)/(4 \times 4)$ Pb/Cu(111) structure, and the plotted plane is vertical to the Cu(111) surface and along the longer diagonal of the parallelogram pattern (in Fig. 3a); **b** the same as **a**, but the plotted plane is parallel to the Cu(111) surface and

crossing the Pb atoms in the second layer. Solid lines (red area indicates highest value) and dashed lines (blue area indicates lowest value) correspond to $\Delta\rho > 0$ and $\Delta\rho < 0$, respectively. The white area corresponds to $\Delta\rho = 0$

Fig. 6 **a** The eight important sites of Ge atom adsorption on $(2 \times 2)/(3 \times 3)$ Pb/Cu(111) surface, and the green parallelogram shows one super cell; **b** the total energies and **c** the binding energies of the eight important adsorption systems of Ge atom on $(2 \times 2)/(3 \times 3)$ Pb/Cu(111) surface



Conclusions

In summary, we find a stable periodic strain-relief template by using energy minimizations with the MD calculations and the self-consistent first-principles calculations. The $(2 \times 2)/(3 \times 3)$ and $(3 \times 3)/(4 \times 4)$ Pb bilayer/Cu(111) are stable structures among the $[(n-1) \times (n-1)]/(n \times n)$ Pb bilayer/Cu(111) ($n = 2, 3, \dots, 12$) structures, which are calculated with MD simulations based on Chen-Möbius inversion potential. However, first-principles calculations show that the $(3 \times 3)/(4 \times 4)$ Pb bilayer/Cu(111) is fully covered by Pb atoms with almost (1×1) atomic and electronic structures on the surface of Pb bilayer, and thus it is not suitable to be used as a periodic template. For

the $(2 \times 2)/(3 \times 3)$ Pb bilayer/Cu(111) stable structure, the ordered Pb semi-clusters are found to show a high-density array on the first Pb atoms layer, and the high and zero electron charge density areas periodically locate in the second Pb layer. These different areas with different atomic and electronic structure will lead to the selective adsorption of atoms on the surface of $(2 \times 2)/(3 \times 3)$ Pb bilayer/Cu(111) structure. The further calculations on the eight adsorption sites of Ge atoms on $(2 \times 2)/(3 \times 3)$ Pb bilayer/Cu(111) structure also confirm this conclusion. Ge atoms prefer to adsorb on the S3, S4 and S6 sites. This stable periodic template can be realized under certain experimental conditions. As a result, the strain-relief periodic $(2 \times 2)/(3 \times 3)$ Pb bilayer/Cu(111) structure is a

promising candidate for the new self-organized template to assemble ordered quantum dots on it with a very high density, and may be one of the new platforms for studying next-generation microelectronics. Our method may be useful for the search of other stable templates for quantum structure arrays, that is, superlattice of nanostructures with size and period much smaller than the wavelength of an electron.

Acknowledgments We thank Prof. Qi-Kun Xue and Yu-Gui Yao for very helpful discussions. The work at Tsinghua University was supported by the Nature Science Foundation of China (NSFC, No. 50531050), the 973 Project (No.2006CB605100), and China Postdoctoral Science Foundation funded project (No. 20090450426). The work of YZ was partially supported by CRI of UNC-Charlotte.

Open Access This article is distributed under the terms of the Creative Commons Attribution Noncommercial License which permits any noncommercial use, distribution, and reproduction in any medium, provided the original author(s) and source are credited.

References

1. J.V. Barth, G. Costantini, K. Kern, *Nature* **437**, 671 (2005)
2. H. Brune, M. Giovannini, K. Bromann, K. Kern, *Nature* **394**, 451 (1998)
3. X.C. Wang, Q. Lin, R. Li, Z.Z. Zhu, *Phys. Rev. B* **73**, 245404 (2006)
4. X.C. Wang, Z.Z. Zhu, *Phys. Rev. B* **75**, 245323 (2007)
5. S.C. Li, J.F. Jia, R.F. Dou, Q.K. Xue, I.G. Batyrev, S.B. Zhang, *Phys. Rev. Lett.* **93**, 116103 (2004)
6. K. Wu, Y. Fujikawa, T. Nagao, Y. Hasegawa, K.S. Nakayama, Q.K. Xue, E.G. Wang, T. Briere, V. Kumar, Y. Kawazoe, S.B. Zhang, T. Sakurai, *Phys. Rev. Lett.* **91**, 126101 (2003)
7. M. Renzhi, W. Yang, T.E. Mallouk, *Small* **5**, 356 (2009)
8. D. Vanderbilt, *Surf. Sci.* **268**, L300 (1992)
9. Y. Yafet, E.M. Gyorgy, *Phys. Rev. B* **38**, 9145 (1988)
10. V.I. Marchenko, *JETP Lett.* **33**, 381 (1981)
11. O.L. Alerhand, D. Vanderbilt, R.D. Meade, J.D. Joannopoulos, *Phys. Rev. Lett.* **61**, 1973 (1988)
12. B. Diaconescu, T. Yang, S. Berber, M. Jazdzyk, G.P. Miller, D. Tomanek, K. Pohl, *Phys. Rev. Lett.* **102**, 56102 (2009)
13. C. Didiot, A. Tejeda, Y. Fagot-Revurat, V. Repain, B. Kierren, S. Rousset, D. Malterre, *Phys. Rev. B* **76**, 81404 (2007)
14. N.X. Chen, *Phys. Rev. Lett.* **64**, 1193 (1990)
15. Y. Long, N. X. Chen, *J. Phys. Condens. Mat.* **19** (2007)
16. Y. Long, N.X. Chen, *Comp. Mater. Sci.* **42**, 426 (2008)
17. Y. Long, N.X. Chen, *Comp. Mater. Sci.* **44**, 721 (2008)
18. N.X. Chen, Z.D. Chen, Y.C. Wei, *Phys. Rev. E* **55**, R5 (1997)
19. X.C. Wang, Y. Jia, Q. Yao, F. Wang, J.X. Ma, X. Hu, *Surf. Sci.* **551**, 179 (2004)
20. R. van Gastel, R. Plass, N.C. Bartelt, G.L. Kellogg, *Phys. Rev. Lett.* **91**, 55503 (2003)
21. G. Kresse, J. Furthmuller, *Comp. Mater. Sci.* **6**, 15 (1996)
22. G. Kresse, J. Furthmuller, *Phys. Rev. B* **54**, 11169 (1996)
23. G. Kresse, J. Hafner, *Phys. Rev. B* **47**, 558 (1993)
24. J.P. Perdew, Y. Wang, *Phys. Rev. B* **45**, 13244 (1992)
25. J.P. Perdew, J.A. Chevary, S.H. Vosko, K.A. Jackson, M.R. Pederson, D.J. Singh, C. Fiolhais, *Phys. Rev. B* **46**, 6671 (1992)
26. H.J. Monkhorst, J.D. Pack, *Phys. Rev. B* **13**, 5188 (1976)
27. M.C. Payne, M.P. Teter, D.C. Allan, T.A. Arias, J.D. Joannopoulos, *Rev. Mod. Phys.* **64**, 1045 (1992)
28. P. Monachesi, L. Chiodo, R. Del Sole, *Phys. Rev. B* **69**, 165404 (2004)
29. M.E. Gonzalez-Mendez, N. Takeuchi, *Phys. Rev. B* **58**, 16172 (1998)